Palaeoenvironmental reconstruction of Hüsamlar coal seam, SW Turkey

Zeynep Büçkün[1], Hülya İnaner[1], Rıza Görkem Oskay[2] and Kimon Christanis[2,*]

[1]*Department of Geological Engineering, Dokuz Eylül University, Buca-Tınaztepe Campus, Buca-İzmir, Turkey.*
[2]*Department of Geology, University of Patras, 265.04 Rio-Patras, Greece.*
[*]*Corresponding author. e-mail: christan@upatras.gr*

The Ören and Yatağan Basins in SW Turkey host several Miocene coal deposits currently under exploitation for power generation. The present study aims to provide insight into the palaeoenvironmental conditions, which controlled the formation of the Hüsamlar coal seam located in Ören Basin. The coal seam displays many sharp alternations of matrix lignite beds and inorganic, lacustrine sediment layers. The coal is a medium-to-high ash lignite (10.47–31.16 wt%, on dry basis) with high total sulphur content (up to 10 wt%, on dry, ash-free basis), which makes it prone to self-combustion. The maceral composition indicates that the peat-forming vegetation consisted of both arboreal and herbaceous plants, with the latter being predominant in the upper part of the seam. Mica and feldspars contribute to the low part of the seam; carbonates are dominant in the upper part, whereas quartz and pyrite are present along the entire coal profile. The sudden transitions of the telmatic to the lacustrine regime and reverse is attributed to tectonic movements that controlled water table levels in the palaeomire, which affected surface runoff and hence, clastic deposition.

1. Introduction

During the Late Cenozoic, an extensional tectonic regime dominated the southwestern part of Turkey resulting in the formation of several NW–SE and NE–SW trending graben systems such as those of the Büyük Menderes, Denizli, Söke, Yatağan, Ören, and Karacasu (Yılmaz *et al.* 2000; Alçiçek 2010). Coeval with these tectonic events, the environment, geological, and climatic conditions favoured peat accumulation resulting in the formation of major coal deposits mostly during the Miocene (İnaner and Nakoman 1997; Oskay *et al.* 2014).

The Yatağan and Ören Basins (figure 1), the latter also called, the Milas Basin, are the most important coal-bearing basins in SW Turkey. Both basins occupy an area of about 350 km^2 and host several coal deposits totalling about 405 Mt mineable reserves. The deposits are exploited from surface and underground mining; the annual production of 13.1 Mt (Turkish Coal Enterprise 2013) supplies three thermal power plants, namely those of Yatağan, Yeniköy and Kemerköy (figure 1), with a total installed capacity of 1680 MW (Querol *et al.* 1999; İnaner *et al.* 2008).

In the last decades, research focused on geological and palaeoenvironmental features of Yatağan and Ören Basins (Nebert 1957; Becker-Platen 1970; Benda 1971; Ünal 1988; Seyitoğlu and Scott 1991; Yılmaz *et al.* 2000; Gürer and Yılmaz 2002; Kayseri-Özer *et al.* 2014) or on mineralogical and petrological features, mainly feeding coal to the power plants (Querol *et al.* 1999; Toprak 2009;Fotopoulou *et al.* 2010; Akar *et al.* 2013). No detailed coal-petrological study of the seams in the above-mentioned basins has been performed up to now.

Keywords. Lignite; coal petrology; depositional environment; Muğla; Ören Basin.

J. Earth Syst. Sci. **124**, No. 4, June 2015, pp. 729–746

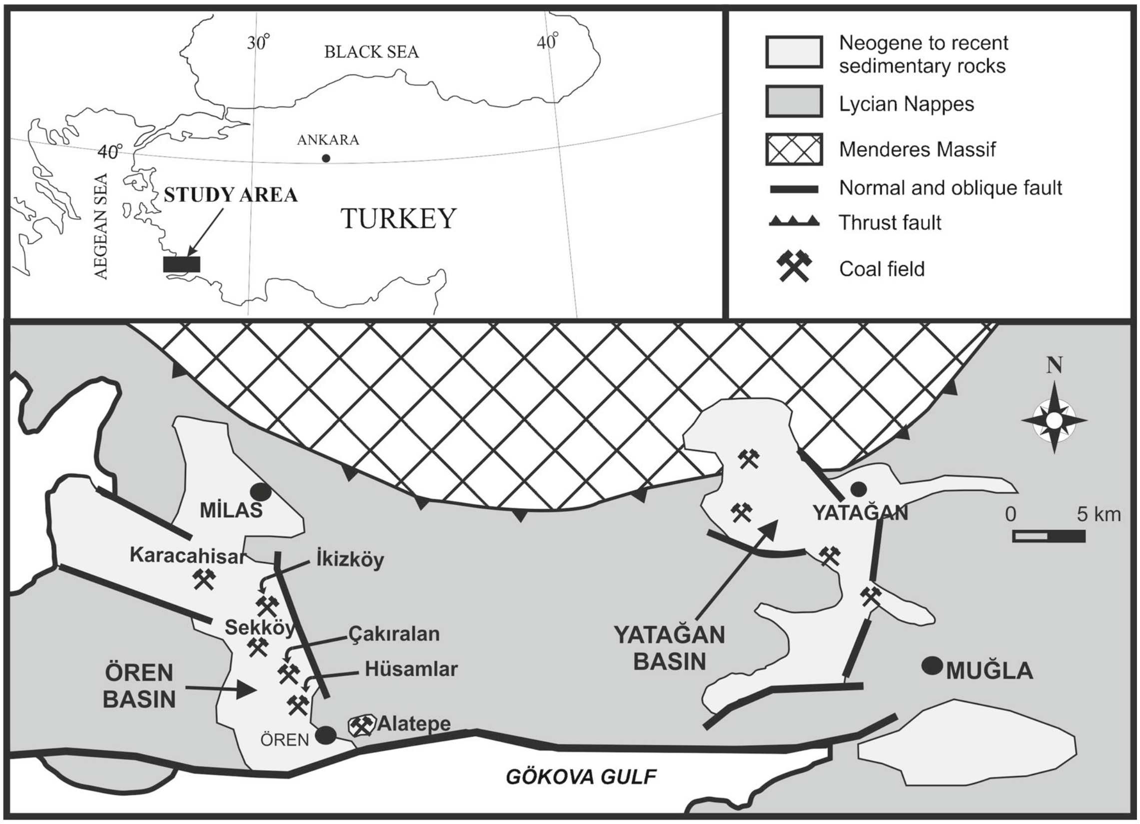

Figure 1. Simplified location and geological map of the study area (modified from İnaner and Nakoman 2001; Gürer and Yılmaz 2002; Alçiçek 2010).

The present study deals with the Hüsamlar coal seam hosting around 51 Mt mineable reserves and supplying the Kemerköy Power Plant (Büçkün 2013). The main objective of this paper is to set out the factors controlling coal formation and to reconstruct the palaeoenvironmental conditions during peat accumulation using petrographic and mineralogical data.

2. Geological setting

The Ören Basin is a NNW–SSE oriented 19-km long and 14-km wide basin in SW Turkey (Yılmaz *et al.* 2000); its surface extends over a 266 km^2 large area at altitudes between +50 m and +1000 m above sea level (figure 2). The basin hosts the following coal fields named after the homonymous deposits (from north to south): Karacahisar, Ikizköy, Sekköy, Cakiralan, Hüsamlar, and Alatepe (İnaner *et al.* 2008).

The lithostratigraphical features of basin margins and sedimentary filling are studied by several researchers (Atalay 1980; Seyitoğlu and Scott 1991; Paton 1992; Querol *et al.* 1999; Sun and Karaca 2000; Okay 2001; Collins and Robertson 2003; Gürer *et al.* 2013). The margins and the pre-Neogene basement consist of schist, gneiss, amphibolite, and marble of the Menderes Massif and Lycian Nappes.

The Miocene coal-bearing sequence that unconformably overlays the pre-Neogene basement is subdivided into four formations, namely the Alatepe, Eskihisar, Yatağan, and Milet (figure 3). The Alatepe Formation (Aquitanian-Burdigalian) is ∼200 m thick on average, and consists of mainly mudstone with coal layers deposited under paralic conditions (Atalay 1980; Görür *et al.* 1995). The Alatepe Formation is unconformably overlain by Eskihisar Formation, which comprises Turgut and Sekköy Members (Atalay 1980). The up to 200-m thick Turgut Member consists of alluvial fan deposits (conglomerate alternating with sandstone and mudstone) on the bottom and fluvial deposits (sandstone, siltstone, and mudstone including coal layers) in the upper part. The major coal-bearing Sekköy Member is up to 150 m thick and comprises mudstone, siltstone, marl, and limestone deposited under lacustrine conditions (Atalay 1980; Sun and Karaca 2000; İnaner and Nakoman 2001; Alçiçek 2010). In the Hüsamlar Field, the cumulative coal seam is up to 67 m thick, 35.9 m of which represent the mineable thickness (Gökmen *et al.* 1993; Querol *et al.* 1999). Dating with mammal fossils along with palynological records indicates a Burdigalian–early Tortonian age for the Eskihisar

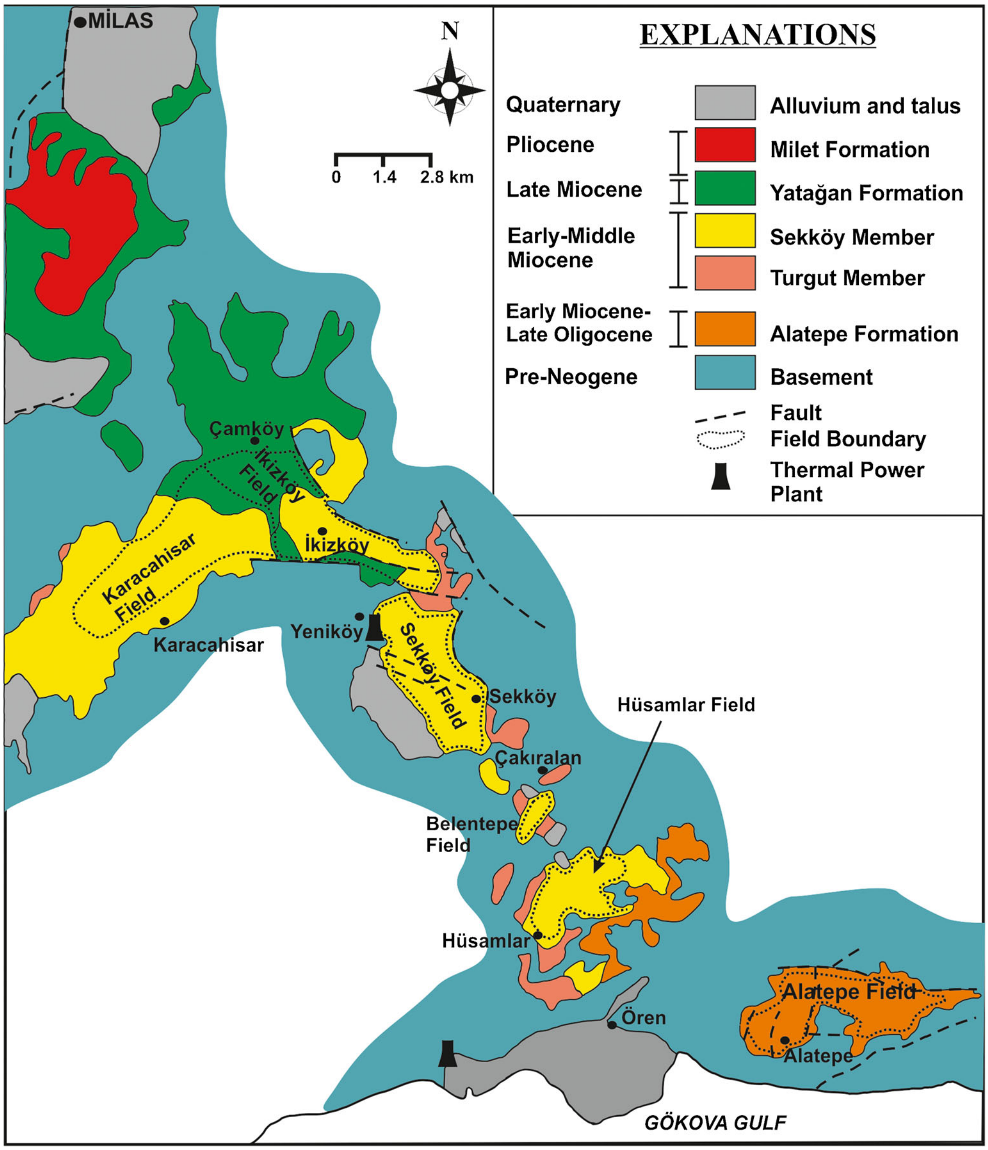

Figure 2. Geological map of Ören Basin (modified from Gökmen *et al.* 1993; Gürer and Yılmaz 2002).

Formation (Becker-Platen 1970; Benda *et al.* 1977; Atalay 1980; Benda and Meulenkamp 1990; Sarac 2003; Akgün *et al.* 2007; Kayseri-Özer *et al.* 2014). The Eskihisar Formation is conformably overlain by the Yatağan Formation (Tortonian-Zanclean; up to 350-m thick) and Milet Formation (Late Zanclean–Gelasian; up to 50-m thick) consecutively. The Milet Formation is lacking in Hüsamlar area (figure 2). Alatepe and Eskihisar formations exist in Hüsamlar Field and are covered by Quaternary alluvial fan and fluvial deposits (Büçkün 2013 and references therein).

3. Materials and methods

Applying channel sampling techniques, 49 (23 coal and 26 inorganic sediment) samples were collected from the Hüsamlar Open Pit. On the basis of the existing mine terraces five sections (A, B, C, D, and E from top to bottom of the seam; see figure 4) were distinguished on the profile; accordingly sampling location coordinates vary between 37°4′31″–37°4′37″N and 27°56′20″–27°56′22″E. The profile was 60-m thick in total (cumulative thickness of coal 20 m) and was logged at site; organic and inorganic layers thinner than 0.5 cm were not separately logged. Coal-lithotype nomenclature followed is consistent with that of the International Committee for Coal and Organic Petrology (ICCP 1993).

Standard proximate and ultimate analyses of all coal samples were performed according to standard procedures (ASTM D3302, D3174, D3175, and D5373 2004). Ultimate analysis was carried out on all the coal samples, using a CARLO ERBA

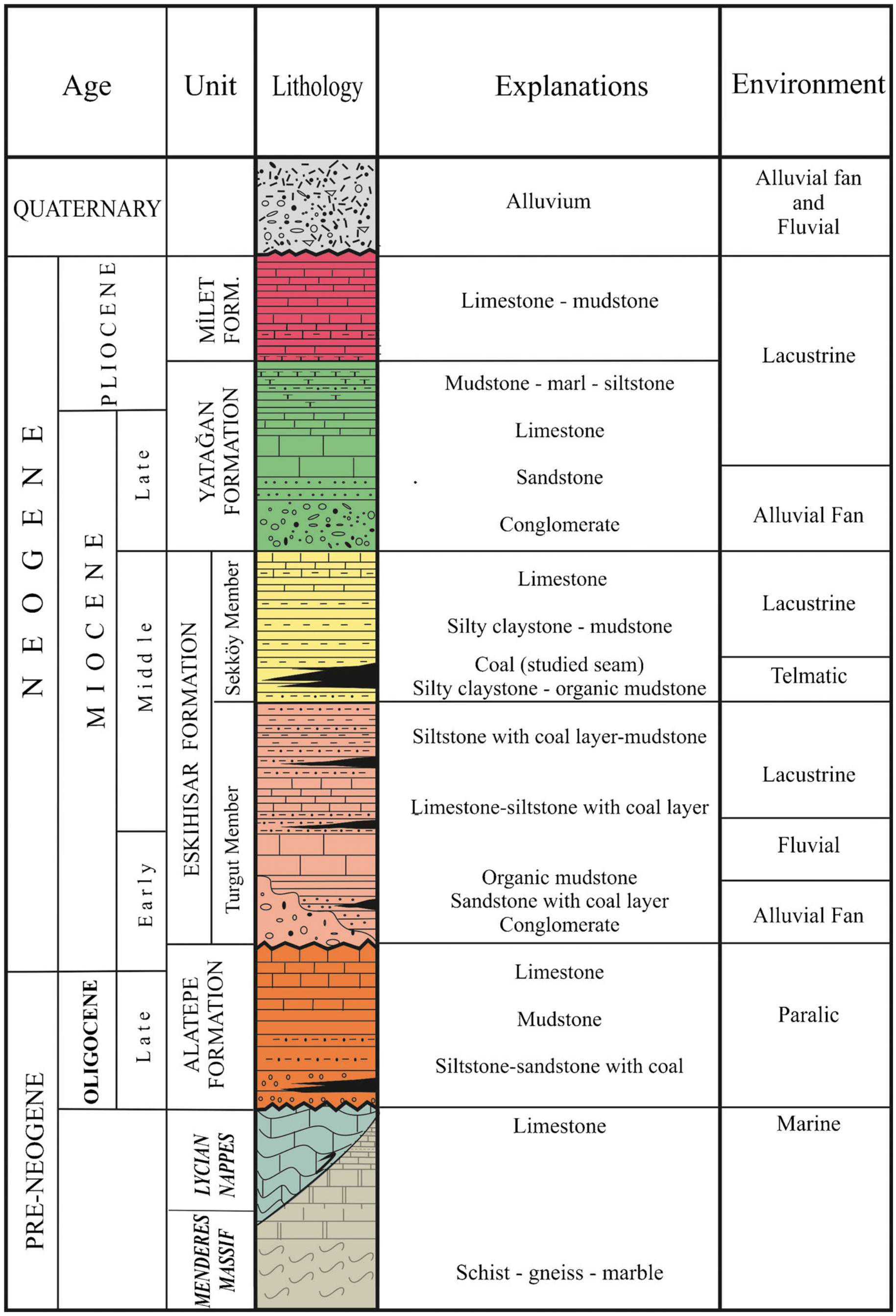

Figure 3. Lithostratigraphical column of Ören Basin (modified from Sun and Karaca 2000).

Automatic Analyzer (EAGER 200) calibrated against the CP1 standard reference material. Gross calorific value was determined in an IKA C5000 adiabatic calorimeter (ASTM D5865 2004).

Polished blocks were prepared from crushed coal according to ISO 7404-2 (2009) and examined under both white incident light and blue-light excitation in oil immersion using a LEICA DMRX coal-petrography microscope. The maceral identification followed the modified Stopes–Heerlen System with the modifications of ICCP System 1994 (ICCP 1971, 2001; Sýkorová *et al.* 2005). Random reflectance of huminite was measured on Eu-ulminite B (ISO 7404-5 2009).

The mineralogical compositions of all coal samples and their ash residues at 750°C, as well as the intercalating inorganic sediment samples were determined using a Bruker D8 Advance X-ray diffractometer equipped with a Lynx-Eye® detector. The scanning area covered the 2θ interval 4–70°, with a scanning angle step of 0.015° and a time step of 1 s. The semi-quantitative determination was performed using Rietveld-based TOPAS software applying the technique described in detail by Siavalas *et al.* (2009).

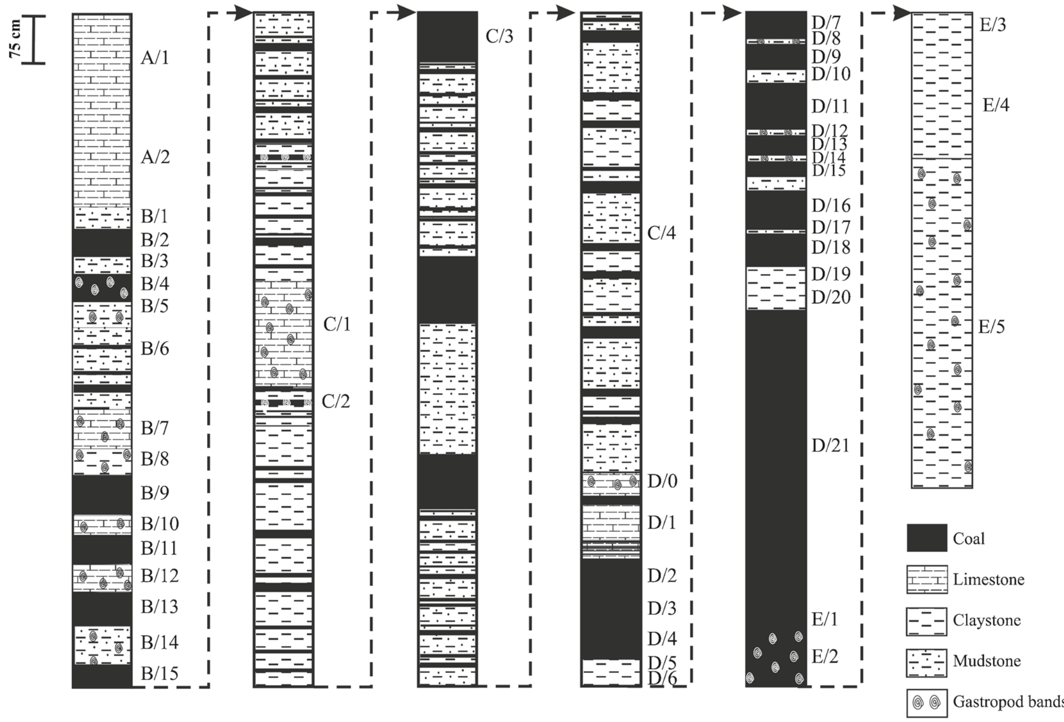

Figure 4. The studied profile at Hüsamlar coal deposit.

Table 1. *The results of proximate and ultimate analyses of Hüsamlar coal samples.*

Sample code	Moisture (wt%)	Ash (wt%, db)	VM (wt%, daf)	CV (MJ/kg, maf)	C	H	N	S	O*	H/C	O/C
					(wt%, daf)						
B/2	19.88	17.02	60.25	21.48	62.31	9.77	1.95	4.79	21.18	1.88	0.25
B/4	19.88	24.25	67.65	17.08	59.48	9.49	2.05	3.17	25.81	1.91	0.33
B/6	22.74	31.16	74.75	17.79	53.96	10.00	2.49	2.26	31.29	2.22	0.43
B/9	20.07	13.97	58.74	20.01	62.33	8.46	1.75	7.96	19.51	1.63	0.23
B/11	22.84	16.98	62.63	19.38	65.40	6.51	1.30	7.48	19.31	1.20	0.22
B/13	23.07	15.13	64.20	19.65	63.64	7.16	1.68	9.74	17.78	1.35	0.21
B/15	23.07	10.47	55.75	22.36	64.07	6.08	1.13	7.75	20.98	1.14	0.25
C/2	20.07	20.10	61.40	18.84	58.07	7.49	1.48	5.40	27.55	1.55	0.36
C/3	20.55	18.34	58.81	19.59	63.26	6.45	1.47	7.89	20.94	1.22	0.25
C/4	22.84	13.15	55.08	20.03	63.38	6.68	2.08	8.88	18.98	1.26	0.22
D/2	19.78	24.92	57.81	19.41	62.32	7.24	2.04	7.82	20.57	1.39	0.25
D/3	17.44	27.71	58.32	19.48	58.38	6.72	1.70	8.08	25.13	1.38	0.32
D/4	13.35	45.20	54.48	17.64	55.29	7.90	2.16	7.05	27.60	1.71	0.37
D/7	18.24	20.22	54.63	18.12	54.59	7.60	1.62	5.94	30.25	1.67	0.42
D/9	22.85	17.23	56.33	19.60	63.29	7.36	2.80	6.44	20.11	1.40	0.24
D/11	24.15	21.62	59.11	18.43	60.53	9.04	2.03	5.00	23.40	1.79	0.29
D/13	19.88	14.07	56.94	20.73	62.59	7.38	1.63	7.31	21.09	1.41	0.25
D/15	16.63	17.36	65.14	22.30	64.47	6.39	1.88	7.74	19.52	1.19	0.23
D/16	23.78	17.89	66.31	19.74	64.00	8.14	2.32	7.29	18.25	1.53	0.21
D/18	19.53	19.69	58.04	20.30	61.49	7.46	1.96	8.15	20.95	1.46	0.26
D/21	18.49	26.87	61.87	20.01	61.82	9.24	2.44	6.45	20.06	1.79	0.24
E/1	20.06	22.84	59.66	20.45	61.50	7.31	1.90	9.84	19.45	1.43	0.24
E/2	22.38	20.67	68.34	19.18	60.01	6.54	1.76	10.34	21.34	1.31	0.27

Note: (db: dry basis; daf: dry ash-free basis; maf: moist ash-free basis; ∗: calculated by subtraction: O = 100–C–H–N–S; atomic ratios H/C and O/C are dimensionless).

4. Results

4.1 *Lithological features*

The total thickness of the coal seam at the sampling site amounts to 60 m; the thickness of the organic layers varies from 0.1 m up to 5 m, whereas the intercalating inorganic sediments (mainly claystone and mudstone) are between 0.5 cm and 5 m thick (figure 4). The profile (particularly sections B and C) displays a 'zebra'-type appearance because of the many alternations of organic and inorganic sediment (massive mudstone) beds. Gastropod remains are frequent in some organic and inorganic strata; freshwater gastropod-rich zones (*Planorbis* spp.) occasionally appearing on the profile, point to sudden rising of water table in the basin.

Macroscopically, the coal has a dark brown to blackish colour and is matt and brittle. Neither xylite layers nor root horizons are included. Matrix is the common lithotype along the studied profile; subordinately, mineral-rich lithotype also occurs. Sulphur mineralization is common in cleats at the bottom of some coal layers. Small coal fragments (∅ < 2 cm) are included in some fine-grained inorganic strata indicating a rather short-distance wash-out of organic matter from mire palaeosurface than erosional activity at a late stage.

Table 2. *Maceral composition (vol.%, on mineral matter-free basis), mineral matter (vol.%, on whole sample), reflectance Rr (%) and palaeoenvironmental indices (dimensionless) of Hüsamlar coal samples.*

Maceral \ Samples	B/2	B/4	B/6	B/9	B/13	C/2	C/4	D/3	D/4	D/7	D/9	D/11	D/13	D/16	D/18	D/21	E/2
Textinite A	1		6	7	6	12	5	1	6	7	3	5		8	4	4	8
Textinite B		1	5	8	6	10	3	1	5	4	2	5		3	3		4
Texto-ulminite A				3	9	5	5	4	6	11	8	6	6	6	8	4	5
Texto-ulminite B				2	6	4	6	1	5	5	4	9		10	7	5	2
Eu-ulminite A	9	8	10	5	5	6	8	14	5	12	14	10	12	9	9	9	12
Eu-ulminite B	20	15	16	5	12	13	17	32	18	18	14	12	22	16	23	31	26
Telohuminite	*30*	*24*	*37*	*30*	*44*	*50*	*44*	*53*	*45*	*57*	*45*	*47*	*40*	*52*	*54*	*53*	*57*
Attrinite	10	18	7	16	6	1		12	19	5	2	8	13	7	9	19	11
Densinite	31	16	22	19	19	27	37	23	16	23	22	19	31	18	19	13	10
Detrohuminite	*41*	*34*	*29*	*35*	*25*	*28*	*37*	*35*	*35*	*28*	*24*	*27*	*44*	*25*	*28*	*32*	*21*
Porigelinite	1	1	2	2	6	1	2	1	2	3	1	3	3	2		1	2
Levigelinite	4	1	4	4	7	5	7	2	2	3	5	3	4	4	3		2
Corpohuminite	2	10	4	7	4	3	2	3	2	2	1	3	1	3	2	2	9
Gelohuminite	*7*	*12*	*10*	*13*	*17*	*9*	*11*	*6*	*6*	*8*	*7*	*9*	*8*	*9*	*5*	*3*	*13*
Huminite	**78**	**70**	**76**	**78**	**86**	**87**	**92**	**94**	**86**	**93**	**76**	**83**	**92**	**86**	**87**	**88**	**91**
Pyrofusinite		1				1	1		1		1			1			
Degradofusinite		1	1	1	1	1			1								
Funginite				1	1				1	1		2				1	1
Semifusinite	2	1	1	1	1	1	1	1	1	1	1	1	1	1	1	1	2
Inertodetrinite	2	1	1	1		1	1		1		5			2	3		
Inertinite	**4**	**4**	**3**	**4**	**3**	**4**	**3**	**1**	**5**	**2**	**7**	**3**	**1**	**4**	**4**	**2**	**3**
Sporinite	4	2	2	1		1					1	1			1		1
Cutinite	7	5	3	1	1	2					1	1	1	2	2	1	
Resinite	1	1	1	1	1	2	1	3.0	2	1	2	3	1	1	3	3	1
Suberinite		5	3	2	2	1	1	1	2		1	2	1	1			2
Alginite	3	4	6	5	4	1	1		2	2	5	3	1	3	1	2	1
Chlorophyllinite				4													
Liptodetrinite	3	9	6	4	3	2	2	1	3	2	7	4	3	3	2	4	1
Liptinite	**18**	**26**	**21**	**18**	**11**	**9**	**5**	**5**	**9**	**5**	**17**	**14**	**7**	**10**	**9**	**10**	**6**
Total org. matter	**100**	**100**	**100**	**100**	**100**	**100**	**100**	**100**	**100**	**100**	**100**	**100**	**100**	**100**	**100**	**100**	**100**
Mineral matter	**7**	**20**	**31**	**3**	**6**	**3**	**3**	**6**	**5**	**7**	**5**	**8**	**3**	**7**	**6**	**6**	**4**
Mean Rr (%)	0.27				0.23				0.28								0.23
St. deviation (±)	0.03				0.03				0.03								0.05
TPI	0.7	0.9	1.2	0.9	1.3	1.6	1.0	1.5	1.2	1.8	1.4	1.5	0.8	1.7	1.7	1.7	2.5
GI	4.7	2.6	3.0	1.4	3.5	2.2	8.7	5.3	1.7	4.5	5.1	3.1	5.6	3.1	4.0	2.8	2.7
GWI	1.1	1.2	1.4	0.8	0.9	0.7	1.1	0.5	0.4	0.6	0.7	0.7	0.8	0.6	0.5	0.3	0.4
VI	0.9	0.8	1.1	0.8	1.6	1.8	1.1	1.6	1.3	1.9	1.3	1.7	0.9	1.8	1.8	1.5	2.7

4.2 *Proximate and ultimate analyses*

Table 1 presents the results of proximate and ultimate analyses of the coal samples. Moisture varies from 13.35 to 24.15%, on as-received basis (avg. 20.50%); the ash yield ranges between 10.47 and 31.16%, on dry basis, with one sample only (D/4) displaying higher value (45.20%). Volatile matter content (VM) averages 60.71% (on dry, ash-free basis), respectively, whereas the gross calorific values vary from 17.08 to 22.36 MJ/kg (on moist, ash-free basis). The elemental composition of lignite proved to average as follows: C 61.14%, H 7.67%, N 1.90%, S 7.08%, and O 22.22% (on dry, ash-free basis). High total S (up to 10.34%, on dry, ash-free basis) and H contents (up to 10%, on dry, ash-free basis) are distinct features of the studied samples; the former can explain the often self-combusting sites at both the coal mine faces and the stockpiles.

4.3 *Coal petrography*

Huminite is the most abundant maceral group varying between 70 and 94 vol.% (table 2, figure 5). Telohuminite and detrohuminite are the most common maceral subgroups with gelohuminite not exceeding 17%. Both varieties of ulminite (texto- and eu-ulminite) constitute up to 51% of the samples. The telohuminite subgroup macerals weakly fluoresce under blue light excitation (textinite A and ulminite A; see figure 6), which might relate to finely dispersed resin that may be present in peat-forming plant material (Suárez-Ruiz *et al.* 1994). The high resin content, in turn, contributes increasing hydrogen content, thus high H/C values (table 1). Such resin-impregnated telohuminite macerals can be related to angiosperms (Sýkorová *et al.* 2005) commonly reported in previous palynological studies in SW Turkey (Benda 1971; Akgün *et al.* 2007;

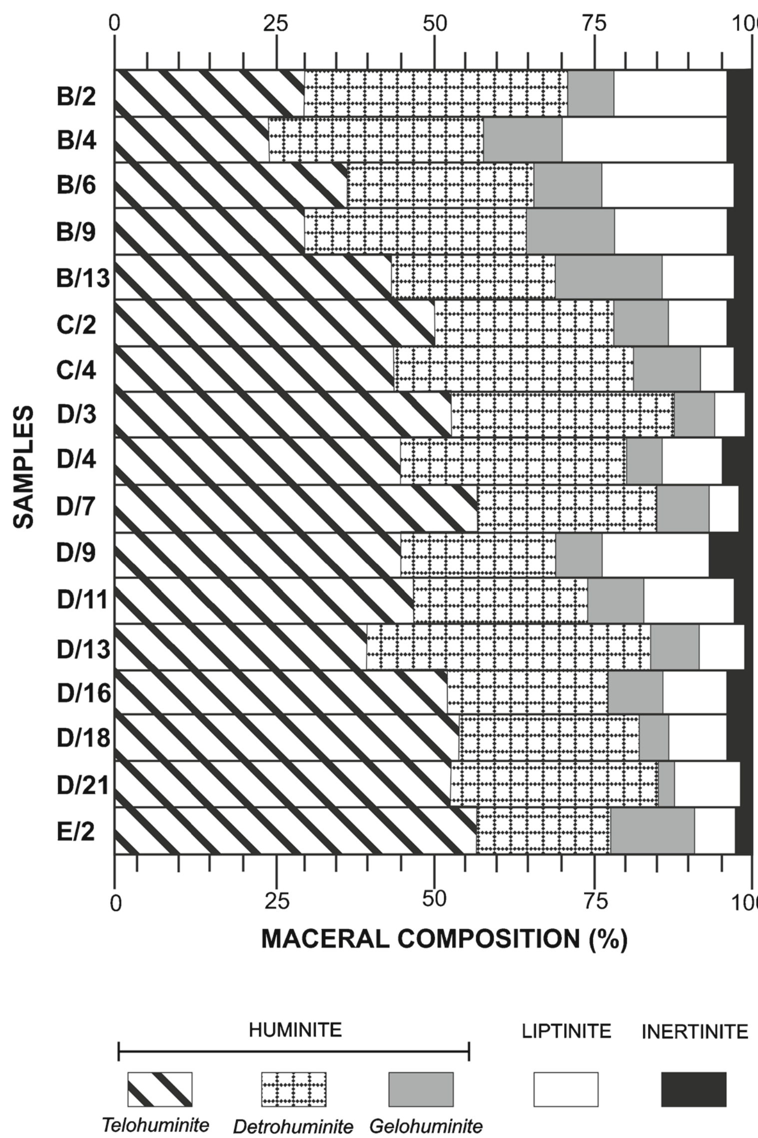

Figure 5. Schematic presentation of the maceral composition (vol.%, on dry, mineral matter-free basis) of the Hüsamlar coal samples.

Kayseri-Özer *et al.* 2014). Detrohuminite sub-group mainly consists of densinite (up to 37%; table 2). Inertinite content is low (<7%); mainly inertodetrinite and semifusinite are present. Liptinite content strongly varies from 5 to 26%. Liptodetrinite and alginite are common, whereas suberinite and resinite display low concentrations (table 2). On the van Krevelen diagram (figure 7), the samples are projected close to sapropelic coal area; however, low alginite content (<6%) does not allow us

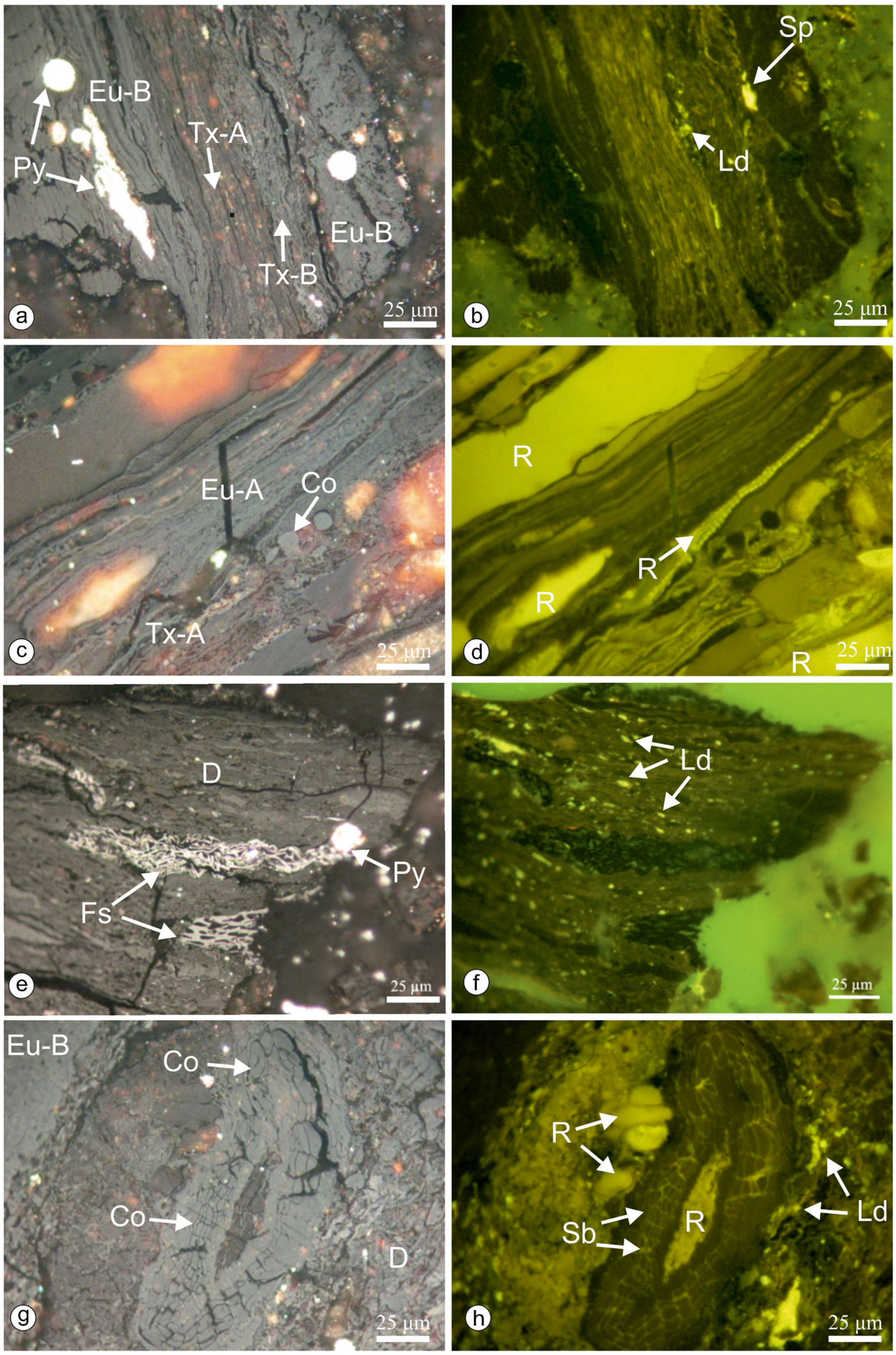

Figure 6. Photomicrographs of Hüsamlar coal: Textinite (Tx), eu-ulminite (Eu), densinite (D), corpohuminite (Co), fusinite (Fs), resinite (R), suberinite (Sb), sporinite (Sp), liptodetrinite (Ld) and pyrite (Py). All photomicrographs are taken under incident white light (**a**, **c**, **e**, **g**) and blue-light excitation (**b**, **d**, **f**, **h**), oil immersion, 500x total magnification.

to consider Hüsamlar coal as sapropelic. Also, oxidised coal particles are rarely observed in the studied samples.

The mineral matter content, as determined using coal-petrography microscopy (table 2), is generally low (<8 vol.%, on whole sample), except for samples B/4 and B/6, which display values about 20 and 31%, respectively. The main minerals determined are framboidal and euhedral pyrite, carbonate, and clay minerals. Huminite random reflectance measured on four lignite blocks varies between 0.23 and 0.28% (table 2).

4.4 *Mineralogical composition*

4.4.1 *Mineral matter in coal*

The evaluation of the X-ray diffractograms indicates that the raw coal samples contain mainly quartz, mica, calcite, pyrite and bassanite (table 3). Taking into account the high organic matter content of the samples, goodness-of-fit (GOF) value <1.5 points to accurate fitting of refinement of crystalline phases. Noteworthy to mention here is that similar mineralogical composition of coal samples from the Muğla Basin is also reported in previous studies (Querol *et al.* 1999; Karayiğit *et al.* 2000; Fotopoulou *et al.* 2010).

Quartz is the most common mineral in all samples ranging between 9.0 and 57.9 wt% of the crystalline mineral matter. It is generally considered being of detrital origin in coal (Ruppert *et al.* 1991; Ward 2002; Dai *et al.* 2008). However, quartz is not confirmed by the microscopic examination of the Hüsamlar lignite samples. The latter was also reported by Querol *et al.* (1999) for coal samples from Muğla Basin, that even though quartz was not determined under the microscope, it appeared

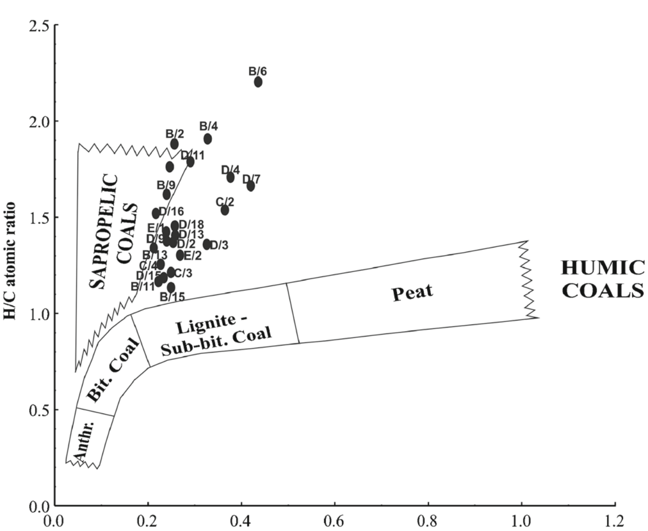

Figure 7. The van Krevelen diagram of the Hüsamlar coal samples (maturity fields after Killops and Killops 1993).

on the XRD reflectograms. Silica gel filling cavities might be related with dissolution of quartz or Si from organic matter pointing to alkaline conditions. These siliceous solutions might have been re-precipitated in the palaeomire under acidic conditions (Stach *et al.* 1982).

Mica is another common silicate mineral contained in values between 13.2 and 65.1 wt% in the C, D, and E sections only (table 3). This may suggest that mica along with chlorite, which can be derived from mica alteration (Diessel 1992; Dai and Chou 2007; Kostova and Zdravkov 2007; Dai *et al.* 2008), were transported into the palaeomire as clastic input during high runoff. High total silicate contents (>76 wt%; see table 3) can be related to medium to high detrital tendencies (Vassilev and Vassileva 2009). Siliciclastic or crystalline rocks in the surrounding area such as sandstone, schist, amphibolites, etc. (figure 2), are obvious sources for detrital mica and quartz supply.

Pyrite is common along the entire profile (up to 72 wt% of the crystalline phases). It forms syngenetically in peat through the reaction of dissolved Fe ions with H_2S derived from bacterial reduction of sulphate-rich waters entering the palaeomire (Casagrande *et al.* 1980; Querol *et al.* 1989; Chou 2012; Kolker 2012). Clay minerals or micas could be the source of dissolved iron; on the other hand, sulphate-rich waters can be supplied by karstic aquifer in this area (Baba *et al.* 2003). Framboidal pyrite crystals are typical for such reducing conditions (Querol *et al.* 1989; Kortenski and Kostova 1996; Kolker 2012).

Calcite (up to 74.8 wt%) can generally be emplaced as clastic input from carbonate rocks (limestone or marble) or authigenically as cleat infillings. Under the microscope, the Hüsamlar samples proved lacking in sharp-angular calcite fragments; this suggests a rather authigenic origin. Calcareous material in cleats, gastropod-bearing samples and intercalation with carbonate-rich strata are common. Aragonite of syngenetic origin is only observed in three samples (B/2, B/4 and B/6), all of which are hosted in the upper part of the profile. The lack of aragonite in the gastropod-bearing samples (table 3) can be explained through calcite transformation during peat accumulation or after burial under neutral to acidic pH conditions (Kortenski 1992; Querol *et al.* 1999; Karayiğit *et al.* 2000). Presence of shell-rich bands with high calcite contents and very low or trace amounts of aragonite are common in Neogene coal seams hosted in intermontane basins of Turkey (Karayiğit *et al.* 2000). Alkaline conditions were developed within the mire and additional Ca-influx further favoured carbonate precipitation.

Bassanite can derive from partial dehydration of gypsum during coal storage (Ward 2002); it may

Table 3. *Rietveld-based XRD quantification results of Hüsamlar bulk coal samples, in wt.% of the crystalline phases.*

Sample \ Mineral	Aragonite	Calcite	Bassanite	Quartz	Feldspar	Chlorite+ Kaolinite	Mica	Pyrite	GOF
B/2	41.1 (2.4)	43.5 (2.1)		15.4 (2.1)					1.33
B/4	89.4 (0.6)	7.1 (0.4)						3.5 (0.5)	1.22
B/6	77.4 (0.5)	21.4 (0.5)						1.2 (0.2)	1.27
B/9				56.7 (6.1)				43.3 (6.1)	1.33
B/11			42.1 (1.8)	57.9 (1.8)					1.26
C/2		74.8 (0.9)		22.8 (0.8)				2.4 (0.3)	1.23
C/3				49.0 (1.6)	13.4 (1.0)		13.2 (2.3)	24.4 (1.1)	1.26
D/2			6.6 (0.5)	38.8 (1.5)			40.4 (2.0)	14.2 (0.7)	1.26
D/3			10.3 (0.4)	27.7 (0.9)			45.6 (1.6)	16.4 (0.6)	1.19
D/4				25.6 (0.7)	6.0 (0.7)	3.3 (0.5)	65.1 (0.7)		1.26
D/7			27.4 (0.7)	30.2 (1.0)			13.9 (1.4)	28.5 (0.8)	1.11
D/9			11.2 (0.5)	53.0 (1.5)				35.8 (1.3)	1.26
D/11			14.4 (0.8)	9.0 (0.9)	15.3 (1.7)		41.2 (2.7)	20.1 (1.3)	1.21
D/13				28.0 (3.3)				72.0 (3.3)	1.32
D/15		44.1 (1.5)		13.6 (1.9)				42.3 (1.4)	1.26
D/16		7.9 (1.2)		41.0 (2.3)				51.1 (2.2)	1.28
D/18		3.7 (1.8)		39.0 (1.9)				57.3 (2.0)	1.24
D/21				23.0 (1.4)			41.1 (2.4)	35.9 (1.5)	1.20
E/1			6.8 (0.5)	15.2 (1.4)			43.6 (2.8)	34.4 (1.8)	1.22
E/2			43.8 (1.0)	46.6 (1.1)				9.6 (1.5)	1.16

Note: Numbers in parentheses indicate the quantification error; GOF: Goodness-of-fit (see Siavalas *et al.* 2009).

also derive from reaction between sulphuric acid released from pyrite oxidation, and calcite in coal (Rao and Gluskoter 1973). Cleats in some studied samples showed abundant sulphur-bearing mineral (pyrite) filling, which may easily be oxidised; however, bassanite and pyrite occur in the same samples that do not contain calcite (table 3). The lack of any evaporate-bearing formation on the basin margins, as well as the wet conditions (1146–1322 mm mean annual precipation) prevailing in the broad area during Middle Miocene (Kayseri-Özer *et al.* 2014), suggest an epigenetic origin of the sulphate minerals. Previous studies (Querol *et al.* 1999; Karayiğit *et al.* 2000) also reported the presence of gypsum in lignite samples from Hüsamlar and the adjacent deposits and suggested low sulphate concentration but high Ca and organic sulphur contents within the palaeomire; latter can lead to gypsum/bassanite precipitation from pore water (Ward 2002).

Feldspars occur only at minor concentrations in a few samples within the middle part of the profile (table 3). Along with other silicate minerals feldspars appear to be of clastic origin.

Overall, aragonite and calcite occur only in samples that do not contain bassanite, mica, and feldspars, whereas quartz and pyrite are contained in almost all the samples of the profile.

The minerals determined in the 750°C-ash residues are mainly anhydrite, haematite, quartz, and mica (in sections C, D, and E; see table 4). Similar mineral phases are recognised in the bottom and fly ashes of Yatağan and Yeniköy power plants (Fotopoulou *et al.* 2010; Akar *et al.* 2013). Quartz and mica are refractory minerals, whereas anhydrite, haematite, and lime are new phases formed during ashing process. In general, anhydrite derives from dehydrations of bassanite/gypsum (Ward 2002); it can also form through calcite/pyrite reactions (Filippidis *et al.* 1996). The latter case is of minor importance in the Hüsamlar samples as calcite occurs in a few samples only (table 4). Lime mainly derives from calcite and aragonite breakdown (Vassilev and Vassileva 1996; Fernandez-Turiel *et al.* 2004), and haematite from the oxidation of pyrite or other Fe-bearing inorganic constituents (Vassilev and Vassileva 1996; Vassilev *et al.* 2001).

4.4.2 *Mineral matter within intercalations*

The mineralogical composition of the inorganic intercalations is useful to comment on palaeoenvironmental evolution of the site.

Carbonates (calcite and aragonite) dominate in the inorganic layers of the studied profile (table 5), whereas silicates (quartz, feldspars, mica, chlorite/kaolinite) are common in the lower part (sections D and E). Pyrite and gypsum occur occasionally throughout the profile.

Table 4. *Rietveld-based quantification XRD results of Hüsamlar coal ash, in wt. % of the crystalline phases.*

Sample \ Mineral	Anhydrite	Haematite	Lime	Quartz	Orthoclase	Kaolinite	Chlorite, Albite	Mica	GOF
B/2	89.1 (0.3)	0.7 (0.1)	6.2 (0.1)	2.6 (0.1)	1.4 (0.2)				1.30
B/4	79.1 (0.4)	4.1 (0.3)	15.7 (0.2)	1.1 (0.1)					1.25
B/6	53.9 (0.9)	6.1 (0.4)	39.4 (0.8)	0.6 (0.1)					1.57
B/9	92.1 (0.3)	5.4 (0.2)		2.5 (0.2)					1.21
B/11	89.3 (0.3)	4.6 (0.2)		6.1 (0.2)					1.20
B/13	94.0 (0.3)	4.1 (0.2)		1.9 (0.2)					1.31
B/15	91.7 (0.3)	4.0 (0.2)		4.3 (0.2)					1.23
C/2	79.8 (0.4)	3.4 (0.3)	7.3 (0.2)	9.5 (0.2)					1.21
C/3	60.0 (0.8)	9.7 (0.3)		17.5 (0.4)				12.8 (0.8)	1.12
C/4	90.2 (0.3)	2.8 (0.2)		7.0 (0.2)					1.24
D/2	41.4 (2.5)	11.2 (0.6)		27.8 (1.3)				19.6 (1.5)	1.19
D/3	36.5 (1.8)	14.1 (0.5)		28.2 (0.9)				21.2 (1.5)	1.14
D/4	15.5 (0.4)	1.8 (0.2)		36.3 (0.7)	12.6 (0.6)	7.9 (0.9)	7.0 (0.4)	18.9 (1.1)	1.37
D/7	34.4 (0.9)	27.8 (0.6)		22.0 (0.6)				15.8 (1.4)	1.04
D/9	69.1 (0.9)	10.2 (0.3)		10.0 (0.3)				10.7 (0.9)	1.21
D/11	65.3 (1.2)	12.4 (0.4)		7.3 (0.5)				15.0 (1.3)	1.18
D/13	72.8 (0.9)	14.3 (0.4)		5.2 (0.4)				7.7 (1.0)	1.13
D/15	82.3 (1.0)	12.1 (0.4)	1.0 (0.3)	3.6 (0.3)				1.0 (0.8)	1.15
D/16	79.0 (1.3)	11.4 (0.6)		6.8 (0.4)				2.8 (1.0)	1.16
D/18	67.0 (1.6)	19.2 (0.9)		9.8 (0.6)				4.0 (1.0)	1.11
D/21	44.0 (1.0)	19.1 (0.5)		21.6 (0.6)				15.3 (1.4)	1.21
E/1	52.1 (1.2)	20.4 (0.5)		9.4 (0.5)				18.1 (1.5)	1.12
E/2	65.3 (1.2)	26.6 (0.8)		8.1 (1.1)					1.68

Note: Numbers in parentheses indicate the quantification errors; GOF: Goodness-of-fit (see Siavalas *et al.* 2009).

Table 5. *Qualitative mineral composition of the inorganic intercalations of Hüsamlar coal seam.*

Sample \ Mineral	Ar	Ca	Gy	Py	Hm	Q	Fld	M	Chl+K
A/1	+	+			?				
A/2	+	+			?				
B/1	+	+							
B/3	+	+		?					
B/5	+	+		+					
B/7	+	+		?					
B/8	+	+		?					
B/10		+							
B/12	+	+		?					
B/14	+	+		?					
C/1	+	+							
D/0	+	+		?					
D/1		+							
D/5							+	+	+
D/6			+			+		+	+
D/8	+	+		?					
D/10			+			+	?	+	+
D/12	+	+							
D/14	+	+							
D/17	+	+							
D/19						+	?	+	+
D/20				+		+		+	+
E/3	+	+		+		+			
E/4						+	?	+	+
E/5		+				+	?	+	+

Note: Ar: Aragonite, Ca: Calcite, Gy: Gypsum, Py: Pyrite, Hm: Haematite, Q: Quartz, Fld: Feldspar, M: Mica, Chl: Chlorite, K: Kaolinite.

5. Discussion

5.1 *Rank determination*

Rank determinations of the Hüsamlar coal samples are based on the German and the North American classification schemes (after Taylor *et al.* 1998; see figure 8). Moisture (table 1) cannot be considered a reliable parameter for rank determination of Hüsamlar coal; despite channel sampling, the samples were taken relatively close to the surface and may have lost some water. Random reflectance of huminite (table 2) can only provide a rough rank estimation as it is not totally reliable for low rank coals. Volatile matter content (table 1) is dependent upon the nature of precursor materials in low rank coals (Taylor *et al.* 1998) and the mineral matter contained; for instance, carbonates lose CO_2, clay minerals OH^- and pyrite sulphur. Thus it is obvious for Hüsamlar coal that the high volatile matter contents are connected with high carbonate and pyrite contents (table 3). The C content indicates that the Hüsamlar coal rank is from peat to lignite. For low-rank coals, the gross calorific values serves as a reliable rank parameter (Taylor *et al.* 1998). The range in gross calorific for the Hüsamlar coal indicated a Mattbraunkohle according to the German classification scheme. This would be equal to a rank of lignite to subbituminous coal C using the American system. Of course, the very high S content (table 1) mostly in the form of pyrite (tables 2 and 3), significantly affects the calorific value increasing the heat generated during combustion; thus, the calorific value should be considered with this precaution in mind.

All rank parameters considered, Hüsamlar lignite samples could be classified as sapropelic on the van Krevelen diagram (figure 7). However, the predominance of huminite macerals along with low alginite content and lack of bituminite (table 2) suggest the humic type of Hüsamlar coal. Moreover, the presence of fluorescent telohuminite (resin-impregnated textinite A and ulminite A) pointing to perhydrous coal, cannot be supported because of the strong positive correlation (r =0.77; see figure 9) between total liptinite and H content indicating that high H content might be rather due to liptinite than to fluorescent telohuminite.

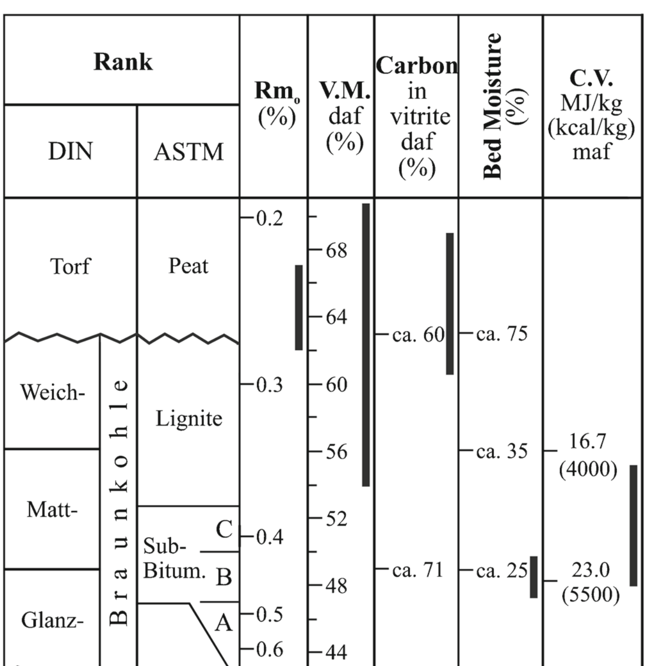

Figure 8. Rank determination of the Hüsamlar coal samples according to the German and the American classification schemes (after Taylor *et al.* 1998).

5.2 *Coal-facies diagrams*

Even though the applicability of maceral ratios and coal-facies diagrams as palaeoenvironmental indicators is debatable (Crosdale 1993; Dehmer 1995; Wüst *et al.* 2001; Scott 2002; Moore and Shearer 2003), they can provide a tool to interpret coal formation when combined with lithostratigraphic, mineralogical, and geochemical data (Kalaitzidis *et al.* 2004, 2010; Siavalas *et al.* 2009; Jasper *et al.* 2010; Zdravkov 2011; Karayiğit *et al.* 2015). The maceral ratios are only indicative and complementary to the sedimentological features for describing and reconstructing the palaeoenvironmental conditions.

The ternary diagram proposed by Mukhopadhyay (1989) provides general information about depositional conditions such as the dominant vegetation type and oxic/anoxic conditions. By plotting the maceral composition (figure 10), almost all samples are projected on the lowest part of the diagram indicating relatively anoxic conditions; this suggests rather high water table in the palaeomire during peat accumulation. The plotting data indicates rather herbaceous vegetation on the palaeomire with tree clusters diminishing towards the upper part of the seam.

The Tissue Preservation Index (TPI) *vs.* Gelification Index (GI) diagram defined by Diessel (1992), and the Groundwater Influence (GWI) *vs.* Vegetation Index (VI) diagram proposed by Calder *et al.* (1991), all based on petrographic data (table 2), are applied to assess conditions during peat accumulation. Both diagrams were proposed firstly for carboniferous coal deposits and were later modified by Kalaitzidis *et al.* (2004) for Tertiary low-rank coals. Moderate to high TPI (0.7–2.5) and GI values (1.4–4.7) characterize Hüsamlar samples indicating good preservation of organic matter along with stable high water level (figure 11). GWI values vary from 0.30 to

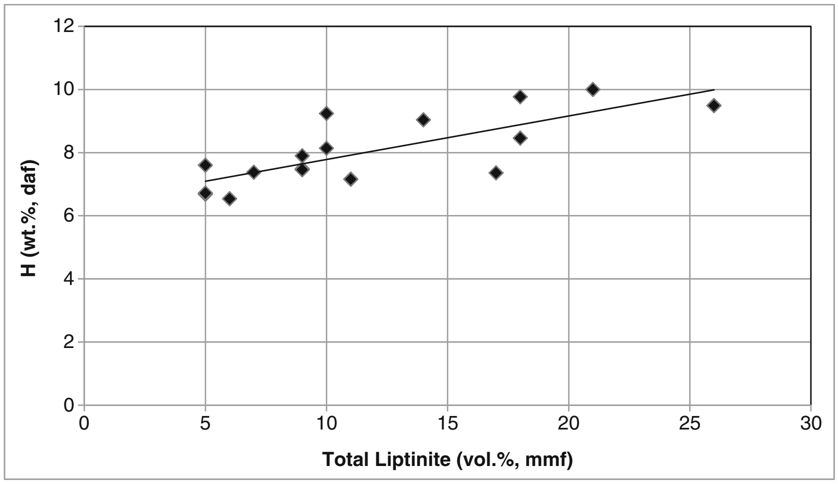

Figure 9. The correlation between liptinite and hydrogen contents in the Hüsamlar coal samples.

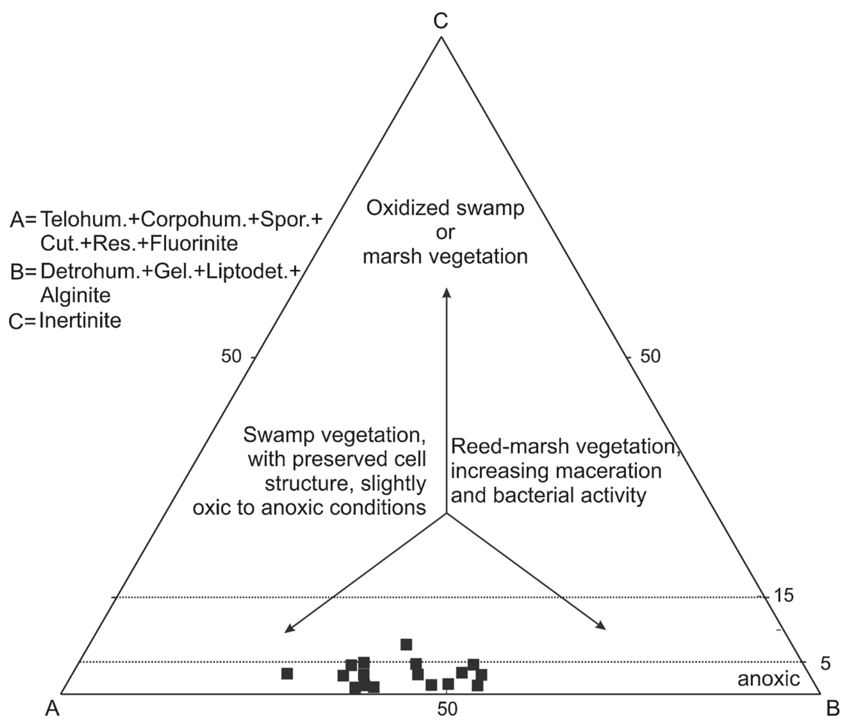

Figure 10. ABC ternary plot of the Hüsamlar coal samples (after Mukhopadhyay 1989).

1.2, whereas VI values range between 0.8 and 2.7 (figure 12). TPI and VI values show distinctly increasing trends from top to bottom of the studied profile (table 2) pointing to an increasing contribution of arboreal species to peat formation towards the floor of the coal seam.

Overall, the above diagrams indicate that the peat at Hüsamlar was accumulating in a limnotelmatic environment, in a fen (topogenous) under mesotrophic, relatively anoxic conditions. The water level was constantly covering the palaeomire surface, hence oxidation was restricted. This wet environment can explain the high well-gelified maceral and the low inertinite contents (figure 5). Herbaceous vegetation prevailed on the palaeomire surface, whereas trees contributed to peat formation in an upward gradually decreasing portion without being dominant.

Similar wet conditions and vegetation changes were reported by Kayseri-Özer *et al.* (2014) who suggest the predominance of herbaceous and woody helophytic vegetation on the Hüsamlar palaeomire under slightly different climatic conditions in comparison with southern parts of Ören Basin. Herbaceous vegetation used to be more common in the upper part of their studied profile. Palaeoflora, as well as mammal fauna suggest narrow open vegetation, which under warm subtropical climate was suitable for mixed-vegetation development on the palaeomire during Middle Miocene. Therefore, mixed detrohuminite and telohuminite dominate in the entire Hüsamlar profile. On the other hand, Ören Basin was narrow in the north during Middle Miocene (Gürer and Yılmaz 2002) and this did not allow the development of a significant mire-forest zone in the area surrounding – located close the basin margins – the palaeomire. Thus, xylite-rich lithotype is missing from the entire studied profile.

5.3 *Palaeoenvironmental reconstruction*

The Ören Basin formed during an extensional tectonic phase, which followed the post-Alpine Orogenese. The filling of the basin began in Late Oligocene–Early Miocene with the deposition of marine sediments such as siltstone, sandstone, mudstone, and limestone (Alatepe Formation). This sequence also hosts a coal seam up to 5.8 m thick, possibly formed under marine influence (Gürer and Yılmaz 2002; Kayseri-Özer *et al.* 2014) and being mineable at Alatepe Field only (Querol *et al.* 1999), at the southernmost part of the Ören Basin (figure 2).

Sedimentation continued with alluvial fan and fluvial deposits (Turgut Member; see figure 3) in Early–Middle Miocene (Becker-Platen 1970; Atalay 1980; Ünal 1988; Querol *et al.* 1999; Alçiçek 2010). Sedimentological and palaeontological data (Akgün *et al.* 2007; Alçiçek 2010; Kayseri-Özer *et al.* 2014)

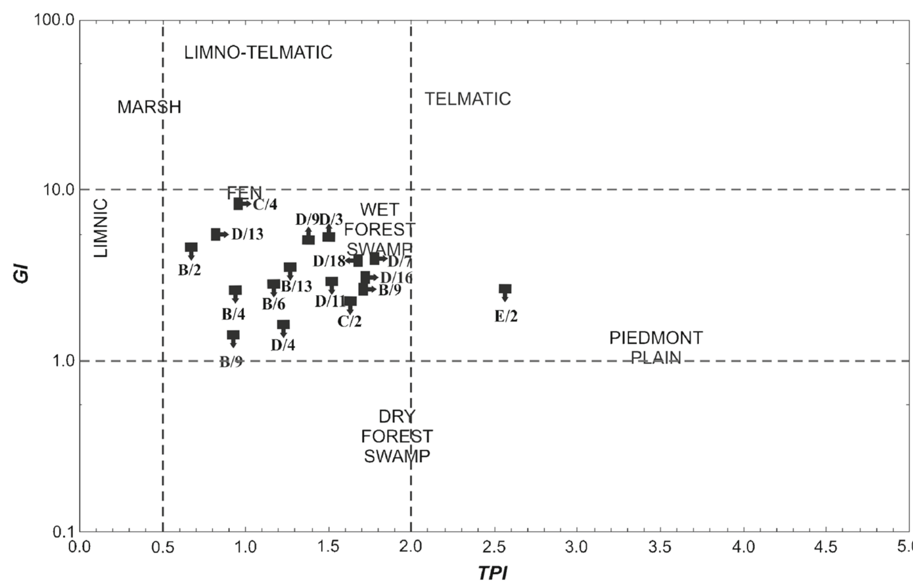

Figure 11. GI *vs.* TPI plot of the Hüsamlar coal samples (after Diessel 1992, as modified by Kalaitzidis *et al.* 2004).

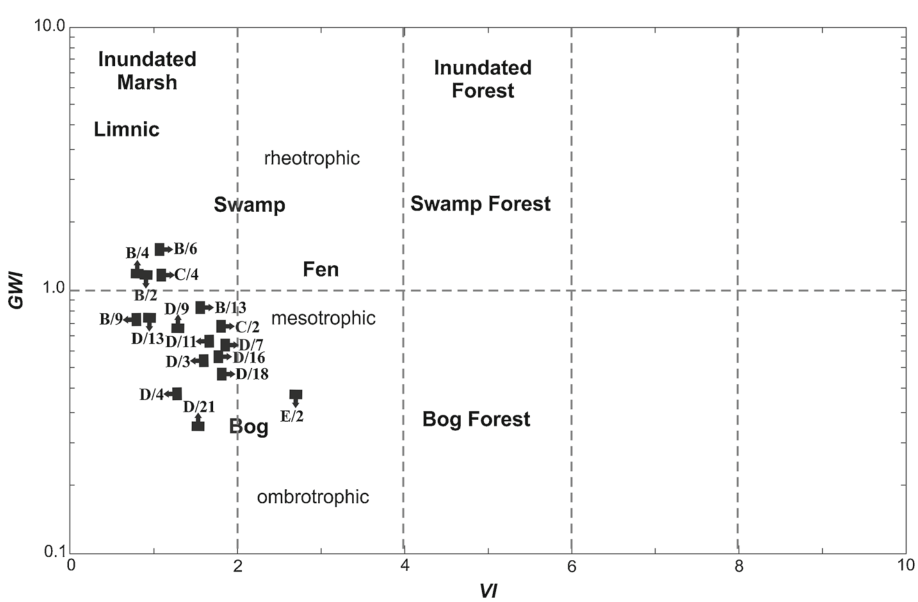

Figure 12. VI *vs.* GWI plot of the Hüsamlar coal samples (after Calder *et al.* 1991, as modified by Kalaitzidis *et al.* 2004).

show that climate changed from semi-arid in the lower part of Turgut Member deposition to warm, humid subtropical during the upper part. In the upper part, the conditions favoured limited peat accumulation and only thin coal layers formed. Conditions became more favourable for lacustrine and telmatic deposits within the Sekköy Member (Middle Miocene) when warm-temperate climate dominated (Akgün *et al.* 2007; Kayseri-Özer *et al.* 2014). Beyond Hüsamlar deposit, in the Ören Basin the İkizköy, Sekköy, and Çakıralan deposits (figure 2) formed with mineable coal seams up to 26.2, 29.9 and 22.6 m thick, respectively (Gökmen *et al.* 1993; Querol *et al.* 1999).

The Hüsamlar coal seam displays a great number of lignite beds intercalating with inorganic sedimentary rocks of exclusively lacustrine origin (figure 4), which points to many alternations of telmatic and lacustrine regimes during this period of time. The initial lake corresponding to the lowest part of section E (E/3-5; see figure 4) was subsequently terrestrialised and telmatic conditions dominated (sections D and upper part of E) with a few, relatively short interruptions only in favour of the lacustrine ones. Quartz, mica, and clay minerals along with calcite and aragonite (table 5) are contained in the inorganic intercalations, whereas mica, quartz, and pyrite dominate in the bulk coal with a few exceptions only (samples D/15 and E2/2; see table 3). Depositional conditions became unstable during the subsequent time interval resulting in several alternations of telmatic and lacustrine conditions (sections B and C); the predominance of carbonates along with some quartz in this part of the studied sedimentary sequence (tables 3, 5) indicate a change in the supply of the palaeomire during the deposition of the upper part of the profile. Finally, peat accumulation ceased and lacustrine limestone deposited (section A). The fact that mica and feldspars contribute to the lignite mineral matter and the inorganic intercalations in the low part of the profile (sections D and E), suggest a differentiation in the origin of the water supplied the palaeomire in the course of time. Christanis (1983) and Kalaitzidis (2007) reported silicate contribution to Philippi peat in the Late glacial part of the profile whereas in the Holocene peat calcite dominated. They explained this difference in the inorganic influx into the Philippi mire with the climatic amelioration and the subsequent karstic-system activation during Holocene. A similar change in the Hüsamlar profile may reflect climatic changes between the time intervals corresponding to the low (sections D and E) and the upper profile parts (sections B, C). Moreover, the sharp contact surfaces between lignite and intercalating layers indicate sudden transitions from telmatic to lacustrine regime and reverse, being rather related with vertical tectonic movements (Yılmaz *et al.* 2000; Gürer and Yılmaz 2002) that resulted in fall or rise, respectively, of the water table in the palaeomire, than with climatic changes.

Palynomorphs and gastropod fossils from Sekköy and Turgut Members indicate freshwater conditions (Querol *et al.* 1999; Kayseri-Özer *et al.* 2014). Despite high S and pyrite concentrations being common in marine-influenced coals, they are also reported from intermontane basins formed during the Alpine Orogenese in circum-Mediterranean mobile belts (e.g., Querol *et al.* 1995; Karayiğit and Whateley 1997; Markic and Sachsenhofer 1997; Taylor *et al.* 1998; Siavalas *et al.* 2009). It seems that sulphur-rich karstic aquifers supplied the palaeomire with freshwater causing neutral to alkaline conditions (Siavalas *et al.* 2009). Moreover, Fe ions derived from clastic inputs (e.g., mica) and/or ferrous iron from degrading plant tissues (Altschuler *et al.* 1983; Chou 2012). Therefore, suitable conditions for sulphur precipitation developed in the palaeomire. Abundance of framboidal pyrite crystals along with calcite points to alkaline conditions during peat formation (Kortenski and Kostova 1996; Querol *et al.* 1995, 1999).

During Late Miocene to Pliocene (Yatağan and Milet Formations) lacustrine conditions dominated in the broad area. However, at Hüsamlar, these formations are lacking probably due to intense erosion and Quaternary alluvial deposits overlying the Middle Miocene sedimentary rocks.

6. Conclusion

The Hüsamlar peat was accumulating in a limnotelmatic environment (topogenous mire), under mesotrophic hydrological and anoxic conditions. The peat-forming vegetation consisted of mainly herbaceous plants with some tree contribution decreasing upwards. The dominance of clastic minerals (mica, quartz) in the low part and that of carbonates in the upper part of the studied coal seam point to a local climatic change during Middle Miocene. On the other hand, sharp transitions from telmatic to lacustrine (and reverse) sediments might be related to tectonic subsidence of the basin. Self-combustion of coal in the mine faces and the stockpiles occurs frecquently; the phenomenon is accelerated due to pyrite oxidation and the bacterial activity.

Acknowledgements

The authors would like to express their gratitude to Mr. Faruk Erin and Mr. N Engin Karaosmanoğlu, TKİ-YLİ (General Directorate of Turkish Coal), Muğla, for the permission and the assistance during field work. For support during laboratory work, special thanks go to Mr. Muzaffer Marçalı, Mr. Mehmet Ali Demirören and Mr. Uğur Yıldız, YLİ, Muğla. Drs George Siavalas, Paraskevi Lampropoulou, Department of Geology, University of Patras and Mr. Dimitrios Vachliotis, Laboratory of Instrumental Analysis, School of Natural Sciences are thanked for carrying out the ultimate analysis. The authors would also like to thank the anonymous reviewers for careful review and valuable comments.

References

Akar G, Sen S, Yılmaz H, Arslan V and Ipekoglu U 2013 Characterization of ash deposits from the boiler of Yenikoy coal-fired power plant, Turkey; *Int. J. Coal Geol.* **105** 85–90.

Akgün F, Kayseri M S and Akkiraz M S 2007 Palaeoclimatic evolution and vegetational changes during the Late Oligocene–Miocene period in the western and central Anatolia (Turkey); *Palaeogeogr. Palaeoclimatol. Palaeoecol.* **253** 56–106.

Alçiçek H 2010 Stratigraphic correlation of the Neogene basins in southwestern Anatolia: Regional palaeogeographical, palaeoclimatic and tectonic implications; *Palaeogeogr. Palaeoclimatol. Palaeoecol.* **291** 297–318.

Altschuler Z S, Schnepfe M M, Silber C C and Simon F O 1983 Sulfur diagenesis in everglades peat and origin of pyrite in coal; *Science* **221** 221–227.

American Society for Testing and Materials (ASTM) D3174 2004 Standard method of ash in the analysis sample of coal and coke from coal; Annual Book of ASTM Standards 2004. Gaseous Fuels: Coal and Coke, vol. 05.06. ASTM, Philadelphia, PA, pp. 322–326.

American Society for Testing and Materials (ASTM) D3175 2004 Standard method of volatile matter in the analysis sample of coal and coke from coal; Annual Book of ASTM Standards 2004. Gaseous Fuels: Coal and Coke, vol. 05.06. ASTM, Philadelphia, PA, pp. 327–330.

American Society for Testing and Materials (ASTM) D3302 2004 Standard method of total moisture in coal; Annual Book of ASTM Standards, Part 26, Gaseous Fuels: Coal and Coke. ASTM, Philadelphia, PA, pp. 352–358.

American Society for Testing and Materials (ASTM) D5373 2004 Standard test methods for instrumental determination of carbob, hydrogen, and nitrogen in laboratory samples of coal and coke; Annual Book of ASTM Standards, Part 26, Gaseous Fuels: Coal and Coke. ASTM, Philadelphia, PA, pp. 504–507.

American Society for Testing and Materials (ASTM) D5865 2004 Standard test method for gross calorific value of coal and coke; Annual Book of ASTM Standards 2004. Gaseous Fuels: Coal and Coke, vol. 05.06, ASTM, Philadelphia, PA, pp. 519–529.

Atalay Z 1980 Stratigraphy of continental Neogene in the region of Muğla–Yatağan, Turkey; *Bull. Geol. Soc. Turkey* **23** 93–99.

Baba A, Kaya A and Birsoy Y K 2003 The effect of Yatağan thermal power plant (Muğla, Turkey) on the quality of surface and groundwaters; *Water, Air, and Soil Pollution* **149** 93–111.

Becker-Platen J D 1970 Lithostratigraphische Unterschungen im Känozoikum Südwest Anatoliens (Türkei) – Känozoikum und Braunkohlen der Turkei; *Beih. Geol. Jb.* **97** 244.

Benda L 1971 Grundzüge einer polenanalytischen Gliederung des türkischen Jungtertiärs (Känozoikum und Braunkohlen der Türkei 4.); *Beih. Geol. Jb.* **113** 46.

Benda L and Meulenkamp J E 1990 Biostratigraphic correlations in the Eastern Mediterranean Neogene 9. Sporomorph associations and event stratigraphy of the Eastern Mediterranean; *Newsletter Stratigraphy* **23** 1–10.

Benda L, Meunlenkamp J E, Schmidt R R, Steffens P and Zachariasse J W 1977 Biostratigraphic correlations in the Eastern Mediterranean Neogene, 2. Correlation between sporomorph associations and marine microfossils from the Upper Oligocene–Lower Miocene of Turkey; *Newsletter Stratigraphy* **6(1)** 1–22.

Büçkün Z 2013 Coal quality of the Muğla–Hüsamlar lignite; Unpubl. MSc Thesis, Dokuz Eylül University, İzmir, Turkey.

Calder J, Gibling M and Mukhopadhyay P 1991 Peat formation in a Westphalian B piedmont setting, Cumberland Basin, Nova Scotia; *Bulletin de la Société Géologique de France* **162(2)** 283–298.

Casagrande D J, Gronli K and Sutton N 1980 The distribution of sulfur and organic matter in various fractions of peat: Origins of sulfur in coal; *Geochim. Cosmochim. Acta* **44** 25–32.

Chou C-L 2012 Sulfur in coals: A review of geochemistry and origins; *Int. J. Coal Geol.* **100** 1–13.

Christanis K 1983 Ein Torf erzählt die Geschichte seines Moores; *Telma* **13** 19–32.

Collins A S and Robertson A H F 2003 Kinematic evidence for Late Mesozoic–Miocene emplacement of the Lycian Allochthon over the western Anatolide Belt, SW Turkey; *J. Geol.* **38** 295–310.

Crosdale P J 1993 Coal maceral ratios as indicators of environment of deposition: Do they work for ombrogenous mires? An example from the Miocene of New Zealand; *Org. Geochem.* **20** 797–809.

Dai S and Chou C-L 2007 Occurrence and origin of minerals in a chamosite-bearing coal of Late Permian age, Zhaotong, Yunnan, China; *Am. Mineral.* **92** 1253–1261.

Dai S, Tian L, Chou C-L, Zhou Y, Zhang M, Zhao L, Wang J, Yang Z, Cao H Z and Ren D 2008 Mineralogical and compositional characteristics of Late Permian coals from an area of high lung cancer rate in Xuanwei, Yunnan, China: Occurrence and origin of quartz and chamosite; *Int. J. Coal Geol.* **76** 318–327.

Dehmer J 1995 Petrological and organic geochemical investigation of recent peats with known environments of deposition; *Int. J. Coal Geol.* **28** 111–138.

Diessel C F K 1992 Coal-bearing depositional systems; Springer-Verlag, Berlin, 721p.

Fernández-Turiel J L, Georgakopoulos A, Gimeno D, Papastergios G and Kolovos N 2004 Ash deposition in a pulverized coal-fired power plant after high-calcium lignite combustion; *Energy & Fuels* **18** 1512–1518.

Filippidis A, Georgakopoulos A and Kassoli-Fournaraki A 1996 Mineralogical components of some thermally decomposed lignite and lignite ash from the Ptolemais basin, Greece; *Int. J. Coal Geol.* **30** 303–314.

Fotopoulou M, Siavalas G, İnaner H, Katsanou K, Lambrakis N and Christanis K 2010 Combustion and leaching behavior of trace elements in lignite and combustion by-products from the Muğla basin, SW Turkey; *Bull. Geol. Soc. Greece,* Proceedings of the 12th International Congress, pp. 2218–2228.

Gökmen V, Memikoğlu O, Dağlı M, Öz D and Tuncalı E 1993 Inventory of Turkish lignites; MTA Publication, Ankara, 356p (in Turkish).

Görür N, Şengör A M C, Sakınc M, Tüysüz O, Akkök R, Yiğitbaş E, Oktay F Y, Barka A, Sarıca N, Ecevitoğlu B, Demirbağ E, Ersoy S, Algan O, Güneysu C and Aykol A 1995 Rift formation in the Gökova region, southwest Anatolia: Implications for the opening of the Aegean Sea; *Geol. Mag.* **132** 637–650.

Gürer Ö F, Sanğu E, Özburanm M, Gürbüz A and Sarica-Filoreau N 2013 Complex basin evolution in the Gökova Gulf region: Implications on the Late Cenozoic tectonics of southwest Turkey; *Int. J. Earth Sci.* **102(8)** 2199–2221.

Gürer Ö F and Yılmaz Y 2002 Geology of the Ören and surrounding areas, SW Anatolia; *Turkish J. Earth Sci.* **11** 1–15.

International Committee for Coal Petrology (ICCP) 1971 International Handbook of Coal Petrography (1st suppl to 2nd edn); Centre National de la Recherche Scientifique, Paris.

International Committee for Coal Petrology (ICCP) 1993 International Handbook of Coal Petrography (3rd suppl to the 2nd edn); Centre National de la Recherche Scientifique, Paris.

International Committee for Coal and Organic Petrology (ICCP) 2001 The new inertinite classification (ICCP System 1994); *Fuel* **80** 459–471.

International Organization for Standardization (ISO) 7404-2 2009 Methods for the Petrographic Analysis of Coals – Part 2: Methods of Preparing Coal Samples; International Organization for Standardization, Geneva, Switzerland, 12p.

International Organization for Standardization (ISO) 7404-5 2009 Methods for the Petrographic Analysis of Coal – Part 5: Method of Determining Microscopically the Reflectance of Vitrinite; International Organization for Standardization, Geneva, Switzerland, 14p.

İnaner H and Nakoman E 1997 Turkish lignite deposits; In: *European Coal Geology and Technology* (eds) Gayer R and Pesek J, *Geol. Soc. Spec. Publ.* **125** 77–99.

İnaner H and Nakoman E 2001 Obtaining various results in coal reserve estimations on Hüsamlar deposit, Muğla-Turkey; Proceedings IESCA 2010, pp. 143–150.

İnaner H, Nakoman E and Karayiğit A I 2008 Coal resource estimation in the Bayir Field, Yatağan–Muğla, SW Turkey; *Energy Sources* **A30** 1000–1015.

Jasper K, Hartkopf-Fröder C, Flajs G and Littke R 2010 Evolution of Pennsylvanian (Late Carboniferous) peat swamps of the Ruhr Basin, Germany: Comparison of palynological, coal petrographical and organic geochemical data; *Int. J. Coal Geol.* **83** 346–365.

Kalaitzidis S 2007 Peat formation and evolution in Greece; Unpubl. PhD Thesis, Dept. of Geology, University of Patras, 350p (in Greek).

Kalaitzidis S, Bouzinos A, Papazisimou S and Christanis K 2004 A short-term establishment of forest fen habitat during Pliocene lignite formation in the Ptolemais Basin, NW Macedonia, Greece; *Int. J. Coal Geol.* **57** 243–263.

Kalaitzidis S, Siavalas G, Skarpelis N, Araujo C V and Christanis K 2010 Late Cretaceous coal overlying karstic bauxite deposits in the Parnassus–Ghiona Unit, Central Greece: Coal characteristics and depositional environment; *Int. J. Coal Geol.* **81** 211–226.

Karayiğit A I and Whateley M K G 1997 Properties of a lacustrine subbituminous (kl) seam, with special reference to the contact metamorphism, Soma, Turkey; *Int. J. Coal Geol.* **34** 131–155.

Karayiğit A I, Gayer R A, Querol X and Onacak T 2000 Contents of major and trace elements in feed coals from Turkish coal-fired power plants; *Int. J. Coal Geol.* **44** 169–184.

Karayiğit A I, Oskay R G, Christanis K, Tunoğlu C, Tuncer A and Bulut Y 2015 Palaeoenvironmental reconstruction of the Çardak coal seam, SW Turkey; *Int. J. Coal Geol.* **139** 3–16.

Kayseri-Özer M S, Akgün F, Mayda S and Kaya T 2014 Palynofloras and vertebrates from Muğla-Ören region (SW Turkey) and palaeoclimate of the Middle Burdigalian–Langhian period in Turkey; *Bull. Geosci.* **89** 137–162.

Kolker A 2012 Minor element distribution in iron disulfides in coal: A geochemical review; *Int. J. Coal Geol.* **94** 32–43.

Kortenski J 1992 Carbonate minerals in Bulgarian coals with different degrees of coalification; *Int. J. Coal Geol.* **20** 225–242.

Kortenski J and Kostova I 1996 Occurrence and morphology of pyrite in Bulgarian coals; *Int. J. Coal Geol.* **29** 273–290.

Kostova I and Zdravkov A 2007 Organic petrology, mineralogy and depositional environment of the Kipra lignite seam, Maritza-West Basin, Bulgaria; *Int. J. Coal Geol.* **71** 527–541.

Markic M and Sachsenhofer R F 1997 Petrographic composition and depositional environments of the Pliocene Velenje lignite seam (Slovenia); *Int. J. Coal Geol.* **33** 229–254.

Moore T A and Shearer J C 2003 Peat/coal type and depositional environment – are they related? *Int. J. Coal Geol.* **56** 233–252.

Mukhopadhyay P 1989 Organic Petrography and Organic Geochemistry of Tertiary Coals from Texas in Relation to Depositional Environment and Hydrocarbon Generation; Report of Investigations, Bureau of Economic Geology, Texas, 118p.

Nebert K 1957 Die Braunkohlenvorkommen von Oeren; Mineral Research and Exploration Institute of Turkey (MTA), Unpubl. Report no 3011, Ankara, 21p.

Okay A I 2001 Stratigraphic and metamorphic inversions in the central Menderes massif: A new structural model; *Int. J. Earth Sci.* **89** 709–727.

Oskay R G, Inaner H, Karayiğit A I and Christanis K 2014 Coal deposits of Turkey: Properties and importance on energy demand; *Bull. Geol. Soc. Greece* **XLVII** 2111–2121.

Paton S 1992 Active normal faulting, drainage patterns and sedimentation in southwestern Turkey; *J. Geol. Soc. London* **149** 1031–1044.

Querol X, Alastuey A, Plana F, López-Soler A, Tuncali E, Toprak S, Ocakoğlu F and Koker A 1999 Coal geology and coal quality of the Miocene Mugla basin, southwestern Anatolia, Turkey; *Int. J. Coal Geol.* **41** 311–332.

Querol X, Chinchon S and Lopez-Soler A 1989 Iron sulfide precipitation sequence in Albian coals from the Maestrazgo Basin, southeastern Iberian Range, northeastern Spain; *Int. J. Coal Geol.* **11** 171–189.

Querol X, Fernández-Turiel J L and Lopez-Soler A 1995 Trace elements in coal and their behaviour during coal combustion in a large power station; *Fuel* **74** 331–343.

Rao C P and Gluskoter H J 1973 Occurrence and distribution of minerals in Illinois coals; Circular, vol. 476, Illinois State Geological Survey, 56p.

Ruppert L F, Stanton R W, Cecil C B, Eble C F and Dulong F T 1991 Effects of detrital influx in the Pennsylvanian Upper Freeport peat swamp; *Int. J. Coal Geol.* **17** 95–116.

Saraç G 2003 Mammal Fossil Findings in Turkey; Scientific Report No. 10609, General Directorate of the Mineral Research and Exploration of Turkey (MTA), Ankara, 208p (in Turkish).

Scott A C 2002 Coal petrology and the origin of coal macerals: Away ahead? *Int. J. Coal Geol.* **50** 119–134.

Seyitoğlu G and Scott B 1991 Late Cenozoic crustal extension and basin formation in west Turkey; *Geol. Mag.* **128** 155–166.

Siavalas G, Linou M, Chatziapostolou A, Kalaitzidis S, Papaefthymiou H and Christanis K 2009 Palaeoenvironment of Seam I in the Marathousa Lignite Mine, Megalopolis Basin (southern Greece); *Int. J. Coal Geol.* **78** 233–248.

Stach E, Mackowsky M, Teichmüller M, Taylor G, Chandra D and Teichmüller R 1982 *Stach's textbook of coal geology*; Gebrüder Borntraeger, Berlin, Stuttgart, 535p.

Suárez-Ruiz I, Jimenez A, Iglesias J, Laggoun-Defarge F and Pradot J G 1994 Influence of Resinite on Huminite Properties; *Energy & Fuels* **8** 1417–1424.

Sun S and Karaca K 2000 Report of geophysical, geological and reserve estimation studies on Muğla, Milas, Hüsamlar and Ekizköy lignite deposits; Report No. 10445, Mineral Research and Exploration Institute of Turkey, MTA, Ankara (in Turkish).

Sýkorová I, Pickel W, Christanis K, Wolf M, Taylor G H and Flores D 2005 Classification of huminite – ICCP System 1994; *Int. J. Coal Geol.* **62** 85–106.

Taylor G H, Teichmüller M, Davis A, Diessel C F K, Littke R and Robert P 1998 *Organic Petrology*; Gebrüder Borntraeger, Berlin, 704p.

Toprak S 2009 Petrographic properties of major coal seams in Turkey and their formation; *Int. J. Coal Geol.* **78** 263–275.

Turkish Coal Enterprise (TKI) 2013 2012 Annual Report, Ankara, 60p (in Turkish).

Ünal D 1988 Geology of Muğla-Milas-Ören-Alatepe Fields; Report, Mineral Research and Exploration Institute, MTA, Ankara (in Turkish).

Vassilev S V, Eskenazy G M and Vassileva C G 2001 Behaviour of elements and minerals during preparation and combustion of the Pernik coal, Bulgaria; *Fuel Processing Technol.* **72** 103–129.

Vassilev S V and Vassileva C G 1996 Occurance, abundance and origin of minerals in coals and coal ashes; *Fuel Processing Technol.* **48** 85–106.

Vassilev S V and Vassileva C G 2009 A new approach for the combined chemical and mineral classification of the inorganic matter in coal. 1. Chemical and mineral classification systems; *Fuel* **88** 235–245.

Ward C R 2002 Analysis and significance of mineral matter in coal seams; *Int. J. Coal Geol.* **50** 135–168.

Wüst R A J, Hawke M I and Bustin M R 2001 Comparing maceral ratios from tropical peatlands with assumptions from coal studies: Do classic coal petrographic interpretation methods have to be discarded? *Int. J. Coal Geol.* **48** 115–132.

Yılmaz Y, Genç Ş C, Gürer F, Bozcu M, Yılmaz K, Karacık Z, Altunkaynak Ş and Elmas A 2000 When did the western Anatolian Grabens begin to develop? In: *Tectonics and magmatism in Turkey and the surrounding area* (eds) Bozkurt E, Winchester J A and Piper J A D, *Geol. Soc. London, Spec. Publ.* **173** 131–162.

Zdravkov A, Bechtel A, Sachsenhofer R F, Kortenski J and Gratzer R 2011 Vegetation differences and diagenetic changes between two Bulgarian lignite deposits – Insights from coal petrology and biomarker composition; *Org. Geochem.* **42** 237–254.

MS received 13 June 2014; revised 13 October 2014; accepted 20 December 2014